Fall Risk Notification System using LiDAR Sensor for the Visually Impaired People

Fall Risk Notification System using LiDAR Sensor for the Visually Impaired People

Daigo Katayama*, Kazuo Ishii, Shinsuke Yasukawa
Graduate School of Life Science and Systems Engineering, Kyushu Institute of Technology,
2-4 Hibikino, Wakamatsu-ku, Kitakyushu-shi, Fukuoka, 808-0135, Japan

Satoshi Nakadomari, Koichi Wada, Akane Befu, Chikako Yamada
NEXT VISION, Kobe Eye Center 2F, 2-1-8, Minatojima, Minamimachi,
Chuo-ku, Kobe-shi, Hyogo, 650-0047, Japan

E-mail: katayama.daigo696@mail.kyutech.jp, ishii@brain.kyutech.ac.jp, s-yasukawa@brain.kyutech.ac.jp,
satoshi.nakadomari@riken.jp, wakichi@nextvision.or.jp, befu@nextvision.or.jp, yamada@nextvision.or.jp.

www.lsse.kyutech.ac.jp

Abstract

We have developed the fall risk notification system using LiDAR sensors to reduce number of fall accidents on platform involving visually impaired people. In this paper, we report the experiment results of the environment recognition algorithm for the fall risk notification system. In this algorithm, height grid map is generated from the depth image from LiDAR sensor and the posture of iPhone. In the experiment, we evaluated the accuracy and responsivity when approaching risky area of falling, such as stairs.

Keywords: Electronic Travel Aids, Negative Obstacle Detection, Point Cloud, LiDAR Sensor.

1. Introduction

Fall Accidents from station platforms are a serious problem in the daily mobility of the visually impaired people. According to statistics[1] from the Ministry of Land, Infrastructure, Transport and Tourism, an average of 76 fall accidents occurs every year, indicating that the number of fall accidents is not small.

To cope with these problems, research and development of devices called electronic walking aids, which convey sensor information in a non-visual way, has been promoted. In recent, smartphones have become a main part of aids, and some have been developed to help people get in line[2] and navigate to their destinations[3]. However, there are few examples of applications that notify the user of the fall risk.

The overview of the electronic walking aid developed in this study is shown in Fig. 1. iPhone 12 Pro processes information about the surrounding environment, and when a warning is needed, it sends a command to the control unit, which vibrates the vibrating device and transmits the information to the user. In this paper, we evaluate the performance of the fall risk notification system using the depth information from LiDAR sensor on the iPhone 12 Pro when the user approaches a risky area of falling.

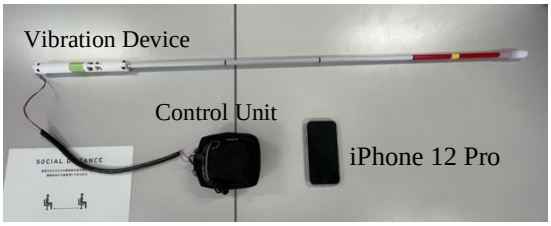

Fig. 1 Overview of the electronic travel aid

2. Methods

2.1. *System Usage Conditions*

This system assumes the usage conditions that the iPhone is tilted by an angle θ and mounted in front of the chest as shown in Fig. 2. Assuming that the height to the user's chest is H_{chest} and the length from the bottom of the iPhone to the camera unit is l_{camera}, the height from the iPhone to the road surface H_{road} is calculated by Eq. (1).

$$H_{\text{road}} = H_{\text{chest}} + l_{\text{camera}} \cos\theta \quad (1)$$

2.2. *Algorithm of Fall Risk Estimation*

This algorithm calculates the risk of falling, the overview shown in Fig. 3. This risk calculates from the minimum distance from the user to a risky area, such as a stair or a gap, and the occupancy of risky area in the user's close range. The details of each step are shown below.

2.2.1. *Conversion from Depth Image to Point Cloud*

3D points $\boldsymbol{p}_{u,v}$ calculate from the depth $d_{u,v}$ obtained from the LiDAR sensor (u, v are coordinates on the depth image) and the intrinsics of the LiDAR sensor (f_u, f_v, c_u, c_v) as shown in Eq. (2).

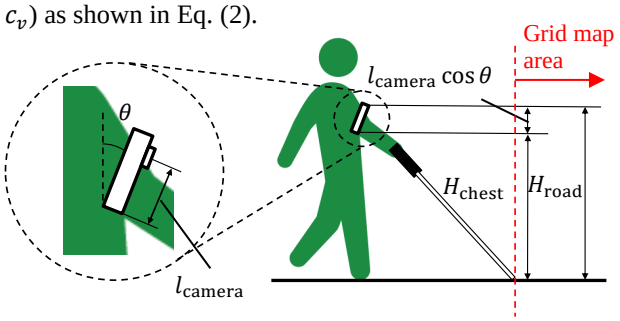

Fig. 2 Mounting position of iPhone

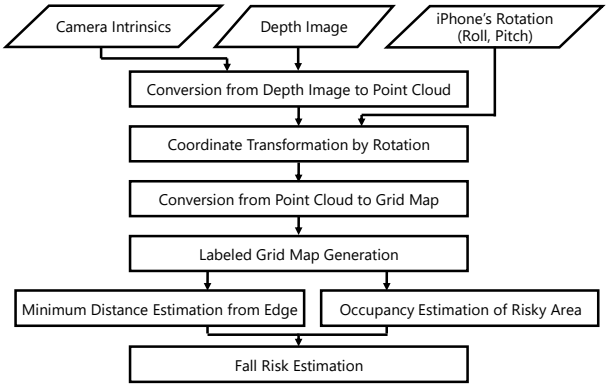

Fig. 3 Overview of fall risk estimation algorithm

$$\boldsymbol{p}_{u,v} = \begin{bmatrix} x \\ y \\ z \end{bmatrix} = \begin{bmatrix} d_{u,v} \\ \frac{u - c_u}{f_u} \\ -\frac{v - c_v}{f_v} \end{bmatrix} \quad (2)$$

2.2.2. *Coordinate Transformation by Rotation*

This method does the coordinate transformation for the points $\boldsymbol{p}$ (camera coordinates) to $\boldsymbol{P}$, the axis indicating the height direction (Z-axis) is in the reverse direction of the gravity direction. this coordinate transformation as shown in Eq. (3) use the quaternion $\boldsymbol{q}$, which is calculated from the Roll angle and Pitch angle of the iPhone. So that the point $\boldsymbol{p}_{u,v}$ and $\boldsymbol{P}_{u,v}$ is set to $\boldsymbol{p}_{u,v}$ = [0, x, y, z], $\boldsymbol{P}_{u,v}$ = [0, X, Y, Z] in Eq. (3).

$$\boldsymbol{P}_{u,v} = \boldsymbol{q}\boldsymbol{p}_{u,v}\boldsymbol{q}^{-1} \quad (3)$$

2.2.3. *Conversion from Point Cloud to Grid Map*

The points $\boldsymbol{P}$ is transformed into the height grid map based on the coordinates in Section 2.1.2 due to reduce the noise in the points and simplify the calculation. The grid stores the points which their X-axis and Y-axis position is inside of the grid range. The height $h_{X,Y}$ (X and Y are coordinates on the grid map) in each grid is calculated from the height (Z-axis position) of the stored point $\boldsymbol{P}$ and the number of stored points n as shown in Ep. (4).

$$h_{X,Y} = \frac{\sum_{k=1}^{n} Z_k}{n} \quad (4)$$

2.2.4. *Labeled Grid Map Generation*

This method generates the labeled grid map by threshold process in order to each grid classify safe and risky areas as shown in Eq. (5). $L_{X,Y}$ is the label of each grid. h_{th} is tolerance of threshold.

$$L_{X,Y} = \begin{cases} Safe\ Area & if\ h_{X,Y} \geq H_{\text{road}} - h_{\text{th}}, \\ Risky\ Area & if\ h_{X,Y} < H_{\text{road}} - h_{\text{th}}. \end{cases} \quad (5)$$

2.2.5. *Minimum Distance Estimation from Edge*

In this method, the labels of the grid are examined along the depth direction (X-axis direction in the grid map) in the grid map, and the edge is defined as the point where the label changes from safe area to risky area. The minimum distance from the edge is calculated by Eq. (6) to the row with the least number of grids to the edge. n_{min} is the least number of grids to the edge, ΔD is the grid width.

$$D_{min} = \Delta D \cdot n_{min} \quad (6)$$

2.2.6. *Occupancy Estimation of Risky Area*

This method calculates the occupancy of the risky area O_{risky} and the occupancy of the safe area O_{safe} in the user's close range by Eq. (7) and (8). n_{risky} and n_{safe} are the number of grids labeled risky area and safe area in closed range. n_{close} is number of grids in closed range.

$$O_{risky} = n_{risky} / n_{close} \quad (7)$$

$$O_{safe} = n_{safe} / n_{close} \quad (8)$$

2.2.7. *Fall Risk Estimation*

The fall risk level is calculated by the minimum distance from the edge and the occupancy of the risky area. The level is classified into three levels as shown below. D_{close} and D_{far} are distance thresholds.

- High level: $D_{min} < D_{close}$ or $O_{risky} > O_{safe}$
- Medium level: $D_{min} > D_{close}$ and $O_{risky} < O_{safe}$
- Low level: $D_{min} > D_{far}$ and $O_{risky} < O_{safe}$

In medium level, add some distance thresholds to be able to notify finely when the minimum distance is updated.

2.3. *Experiment on Risky Area of Fall*

We did the experiment of the system when entering an area where there is a risk of falling. This experiment was done for evaluation the accuracy of the estimation of the minimum distance and the responsivity of the notification. The details are as follows.

2.3.1. *Procedure*

The task of this experiment was for the user to wear the device and walked straight to the goal as shown in Fig. 4. The conditions are as follows.

(i) Approach angle: 90[deg]
(ii) Approach angle: 45[deg]

Condition (i) was assumed that users are getting on and off the train, and condition (ii) was assumed that user are moving along the platform and approaching the edge of the platform.

The data to be collected during the experiment were depth images, attitude and self-position from iPhone.

2.3.2. *Device Setting*

The iPhone was fixed to the front of the user's chest with a harness-type fixture. The iPhone was also tilted forward 30[deg] on the fixture.

2.3.3. *Experiment Place*

This experiment was done on the outdoor at the Wakamatsu campus of Kyushu Institute of Technology. As shown in Fig. 5, this place had a flat surface with a wide stair (Height of step: 0.14[m], Depth of step: 0.34[m]).

2.3.4. *Analysis Method*

The analysis for evaluation were done on the accuracy of the minimum distance and the responsivity of the fall risk notification. For the accuracy of the minimum distance, the error was calculated as the difference between the distance between the start point and the goal point and the distance calculated from the iPhone's self-position and approach angle. The responsivity of the fall risk notification was analyzed by calculating the difference between the time it takes for each level of fall risk to be first presented and calculated distance applied to the estimation of the fall risk level.

This analysis was done on another PC. The PC used for the analysis was MacBook Pro (Made by Apple Inc., CPU: Intel Core i9 (2.3 [GHz], 8 Core), RAM: 16 [GB]), and the software was MATLAB R2021a.

In the analysis, H_{road} = 1.32[m], θ = 30[deg], D_{min} = 1.35[m], D_{far}= 2.35[m], h_{th} = 0.05[m]. The grid width was 0.05[m] in both the X and Y-axis directions, and 1 distance threshold was set 1.85[m].

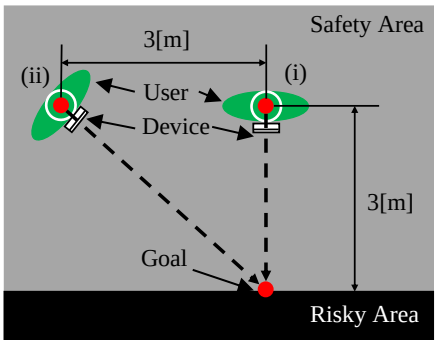

Fig. 5 Conditions of task

Fig. 4 Experiment place

3. Results

3.1. *Accuracy of Minimum Distance from Edge*

The error average of the minimum distance on each condition as shown in Table 1. When approach angle θ_a was 90 [deg], the average errors were less than 5 [%], but when θ_a = 45 [deg], the errors were around 15 [%].

3.2. *Responsivity of Fall Risk Notification*

The difference average in time at the first notification of each fall risk level as shown in Table 2. When the approach angle was $\theta_a = 90$[deg], the differences in time were within the range of ±0.04[s], but when $\theta_a = 45$[deg], the differences were calculated to be around 0.4[s].

4. Discussion

4.1. *Effect of Approach Angle*

In this experiment and analysis, they were shown that the minimum distance from the edge and the time to the first notification of each fall risk level both tended to worsen when the approach angle $\theta_a = 45$[deg].

This cause seems different grid position of the minimum distance from the ideal one when the edges on the grid map do not have a straight-line shape as shown in Fig. 6. This cause effect to the error in the minimum distance by the amount of the grid width, so it is necessary to consider the allowable error including the grid width.

The current algorithm focuses on a single grid point closest to the edge. Therefore, the value of the minimum distance can be unstable, depending on the shape of the edge. The unstable notification can confuse the user[4], we should consider segmentation method such as line fitting for the edge.

Table 1. The error average of the minimum distance

Error average [%]			
Times	1st.	2nd.	3rd.
$\theta_a = 90$ [deg]	5.01	2.20	4.24
$\theta_a = 45$ [deg]	15.0	15.6	15.4

Table 2. The difference in time at the first notification

Difference average in time [s]			
Times	1st.	2nd.	3rd.
$\theta_a = 90$ [deg]	0.034	-0.039	0.028
$\theta_a = 45$ [deg]	0.418	0.445	0.423

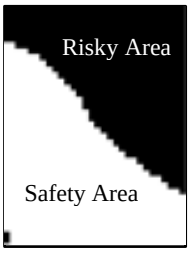

Fig. 6 The shape of the edge on grid map
(In case of $\boldsymbol{\theta_a} = 45$ [deg], 1st.)

4.2. *Challenges in Use by the Visually Impaired*

Based on the results of this experiment, there are two specific issues that need to be considered when considering the actual use of this system by visually impaired people.

The first issue is to stabilize notifications. As mentioned in the previous section, the current algorithm causes unstable notifications when approaching at an angle, i.e., when walking on the platform and approaching the edge of the platform, which may lead to confusion for the user. This issue will be considered in line with the aforementioned.

The second issue is the timing of the notification. As can be seen from Table 2, the timing of notification was found to be later than the ideal one in most cases. Considering the delays caused by the communication with the vibration device and the reaction speed of the user, it is necessary to set a margin for the timing of notification considering the above matters.

5. Conclusion

In this paper, we evaluated an algorithm for the fall risk notification system that visually impaired people of their risk of falling using depth information from LiDAR sensor on iPhone 12 Pro. We mainly evaluated the accuracy of the minimum distance and the responsivity of the notification and found that the above two parameters deteriorated when approaching diagonally to the edge.

In the future, we will try to solve the above problems, and stabilize of notification and implement the notification timing added safety margin.

Acknowledgements

This research was supported by Research Grant of JR–West Relief Foundation in 2020 (Grant No. 20R032).

References

1. MLIT, "Study Group for Improving Safety at Station Platforms", https://www.mlit.go.jp/tetudo/tetudo_fr7_000015.html. (In Japanese)
2. M. Kuribayashi et al., "LineChaser: A Smartphone-Based Navigation System for Blind People to Stand in Lines", Proceedings of the 2021 CHI Conference on Human Factors in Computing Systems, no. 33, pp. 1-13, 2021.
3. M. C. Rodriguez-Sanchez et al., "Accessible smartphones for blind users: A case study for a wayfinding system", Expert Systems with Applications, vol. 41, issue 16, pp. 7210-7222, 2014.
4. M. Tauchi, T. Ohkura, "States and Problems of Assistive Technology for the Visually Impaired: Walking Alone", Journal of the Society of Instrument and Control Engineers, vol. 34, no.2, pp. 140-146, 1995. (In Japanese)

Authors Introduction

Mr. Daigo Katayama

He is a Doctoral Student at Graduate School of Life Science and Systems Engineering, Kyushu Institute of University. He received Master's degree from Graduate School of Life Science and Systems Engineering, Kyushu Institute of University.

Prof. Kazuo Ishii

He is a Professor at Graduate School of Life Science and Systems Engineering, Kyushu Institute of University. He received Ph.D. from School of Engineering, The University of Tokyo.

Dr. Shinsuke Yasukawa

He is an Associate Professor at Graduate School of Life Science and Systems Engineering, Kyushu Institute of University. He received Ph.D. from Graduate School of Engineering, Osaka University.

Dr. Satoshi Nakadomari

He is a Director at NEXT VISION. He graduated from the Department of Medical, The Jikei University. He received Ph.D. from the Department of Medical, The Jikei University.

Mr. Koichi Wada

He is a Vision Park Information Master at NEXT VISION. He graduated from Acupuncture and Physical Therapy Teacher Training School of University of Tsukuba.

Ms. Akane Befu

She is a Vision Park Information Concierge at NEXT VISION. She graduated from The Department of Domestic Science, Tokushima Bunri University.

Ms. Chikako Yamada

She is an Executive Secretary at NEXT VISION. She graduated Graduate School of Sociology, Bukkyo University. She received Master's degree from Graduate School of Sociology, Bukkyo University.